HAL open science

# Contrasting roles of DOP as a source of phosphorus and energy for marine diazotroph

Alba Filella, Lasse Riemann, France van Wambeke, Elvira Pulido-Villena, Angela Vogts, Sophie Bonnet, Olivier Grosso, Julia Diaz, Solange Duhamel, Mar Benavides

## To cite this version:

Alba Filella, Lasse Riemann, France van Wambeke, Elvira Pulido-Villena, Angela Vogts, et al.. Contrasting roles of DOP as a source of phosphorus and energy for marine diazotroph. Frontiers in Marine Science, 2022, 9, 10.3389/fmars.2022.923765 . hal-03787908

**HAL Id: hal-03787908**

**https://hal.science/hal-03787908v1**

Submitted on 27 Sep 2022

**HAL** is a multi-disciplinary open access archive for the deposit and dissemination of scientific research documents, whether they are published or not. The documents may come from teaching and research institutions in France or abroad, or from public or private research centers.

L'archive ouverte pluridisciplinaire **HAL**, est destinée au dépôt et à la diffusion de documents scientifiques de niveau recherche, publiés ou non, émanant des établissements d'enseignement et de recherche français ou étrangers, des laboratoires publics ou privés.

Distributed under a Creative Commons Attribution 4.0 International License

frontiers | Frontiers in Marine Science

ORIGINAL RESEARCH
published: 25 July 2022
doi: 10.3389/fmars.2022.923765

# Contrasting Roles of DOP as a Source of Phosphorus and Energy for Marine Diazotrophs

*Alba Filella[1,2], Lasse Riemann[3], France Van Wambeke[1], Elvira Pulido-Villena[1], Angela Vogts[4], Sophie Bonnet[1], Olivier Grosso[1], Julia M. Diaz[5], Solange Duhamel[1,6] and Mar Benavides[1,2*]*

[1] Aix Marseille Univ, Université de Toulon, CNRS, IRD, Marseille, France, [2] Turing Center for Living Systems, Aix-Marseille University, Marseille, France, [3] Marine Biological Section, Department of Biology, University of Copenhagen, Helsingør, Denmark, [4] Department of Biological Oceanography, Leibniz Institute for Baltic Sea Research, Rostock, Germany, [5] Scripps Institution of Oceanography, University of California San Diego, La Jolla, CA, United States, [6] Department of Molecular and Cellular Biology, The University of Arizona, Tucson, AZ, United States

The oceanic dissolved organic phosphorus (DOP) pool is mainly composed of P-esters and, to a lesser extent, equally abundant phosphonate and P-anhydride molecules. In phosphate-limited ocean regions, diazotrophs are thought to rely on DOP compounds as an alternative source of phosphorus (P). While both P-esters and phosphonates effectively promote dinitrogen ($N_2$) fixation, the role of P-anhydrides for diazotrophs is unknown. Here we explore the effect of P-anhydrides on $N_2$ fixation at two stations with contrasting biogeochemical conditions: one located in the Tonga trench volcanic arc region ("volcano," with low phosphate and high iron concentrations), and the other in the South Pacific Gyre ("gyre," with moderate phosphate and low iron). We incubated surface seawater with AMP (P-ester), ATP (P-ester and P-anhydride), or 3polyP (P-anhydride) and determined cell-specific $N_2$ fixation rates, *nifH* gene abundance, and transcription in *Crocosphaera* and *Trichodesmium*. *Trichodesmium* did not respond to any DOP compounds added, suggesting that they were not P-limited at the volcano station and were outcompeted by the low iron conditions at the gyre station. Conversely, *Crocosphaera* were numerous at both stations and their specific $N_2$ fixation rates were stimulated by AMP at the volcano station and slightly by 3polyP at both stations. Heterotrophic bacteria responded to ATP and 3polyP additions similarly at both stations, despite the contrasting phosphate and iron availability. The use of 3polyP by *Crocosphaera* and heterotrophic bacteria at both low and moderate phosphate concentrations suggests that this compound, in addition to being a source of P, can be used to acquire energy for which both groups compete. P-anhydrides may thus leverage energy restrictions to diazotrophs in the future stratified and nutrient-impoverished ocean.

**Keywords: nitrogen fixation, *Trichodesmium*, *Crocosphaera*, polyphosphate, phosphoanhydride, phosphoester**

OPEN ACCESS

***Edited by:***
*Carol Robinson, University of East Anglia, United Kingdom*

***Reviewed by:***
*Andrew Paul Rees, Plymouth Marine Laboratory, United Kingdom*
*Mitsuhide Sato, Nagasaki University, Japan*

****Correspondence:***
*Mar Benavides*
*mar.benavides@ird.fr*

***Specialty section:***
*This article was submitted to Marine Biogeochemistry, a section of the journal Frontiers in Marine Science*

***Received:*** *19 April 2022*
***Accepted:*** *20 June 2022*
***Published:*** *25 July 2022*

***Citation:***
*Filella A, Riemann L, Van Wambeke F, Pulido-Villena E, Vogts A, Bonnet S, Grosso O, Diaz JM, Duhamel S and Benavides M (2022) Contrasting Roles of DOP as a Source of Phosphorus and Energy for Marine Diazotrophs. Front. Mar. Sci. 9:923765. doi: 10.3389/fmars.2022.923765*

## INTRODUCTION

Phosphorus (P) is an essential nutrient used in cellular components such as nucleic acids, sugars, and lipids (Karl, 2000, 2014; Falkowski, 2001). Long thought to only operate on geological timescales, P is now recognized as a dynamic and microbially-driven cycle with a significant impact on biological productivity and biogeochemical cycling in the ocean (Duhamel et al., 2021). Dinitrogen ($N_2$)-fixing

microbes (so-called diazotrophs) are virtually not nitrogen-limited, which can cause P depletion in the waters where they occur if the required iron levels are met (Wu et al., 2000). Consequently, diazotrophs are highly dependent on P availability (Wu et al., 2000; Sañudo-Wilhelmy et al., 2001; Mills et al., 2004; Webb et al., 2007). However, measurable $N_2$ fixation in P-limited regions suggests that the more abundant reduced P compounds (operationally defined as dissolved organic phosphorus, DOP) may be used by diazotrophs as an alternative source of P (Dyhrman et al., 2007; Palter et al., 2011). Several strategies for exploiting DOP by diazotrophs have been identified, such as the use of specific hydrolytic enzymes (Karl and Björkman, 2015). Marine DOP is a complex and heterogeneous pool, including inorganic, polymeric, and organic compounds grouped according to their P-bonds into three main classes: P-esters, phosphonates, and P-anhydrides (Young and Ingall, 2010; Diaz et al., 2018). The globally important diazotrophs *Trichodesmium* and *Crocosphaera* can grow on P-esters as a sole P source (Dyhrman et al., 2002; Orchard et al., 2003; Dyhrman and Haley, 2006), but only *Trichodesmium* has the genetic machinery needed to leverage P from phosphonates (Dyhrman et al., 2006). Currently, it is not known whether P-anhydrides can serve as a source of P for diazotrophs.

The P-anhydride polyphosphate (polyP) provides microbial cells with stress protection, nutrient deficiency acclimation, and cell signaling properties, among many other functions (Sanz-Luque et al., 2020). Several phytoplankton groups can obtain P from polyP (Björkman and Karl, 1994; Moore et al., 2005; Diaz et al., 2016), and some marine diatoms may even prefer polyP over the more abundant P-esters (Diaz et al., 2019). However, the role of P-anhydrides in marine microbial productivity and biogeochemical cycling remains uncertain (Martin et al., 2014; Li and Dittrich, 2019), particularly for diazotrophs, which thrive primarily in P-limited regions of the global ocean. Key diazotrophs such as *Trichodesmium* and *Crocosphaera* are genetically equipped to produce and degrade polyP (*ppK* and *ppX* genes; Dyhrman and Haley, 2006; Orchard et al., 2010b). To our knowledge, no studies have examined the role of polyP in $N_2$ fixation.

Projected changes in surface ocean stratification, atmospheric deposition, and ocean ventilation can reduce phosphate supply in the future (e.g., Kemena et al., 2019; Duhamel et al., 2021). Such changes may cause a shift in nutrient availability from oxidized toward more reduced organic compounds recycled through the upper ocean. Thus, the ability of diazotrophs to exploit different DOP compounds as an alternative source of P may influence their activity and distribution in the future warm and stratified ocean, potentially impacting nitrogen inputs, biological productivity, and carbon sequestration (Dyhrman et al., 2007). Here we assess the role of P-anhydrides in $N_2$ fixation by *Trichodesmium* and *Crocosphaera* at two stations in the Western South Pacific characterized by contrasting phosphate availability.

## MATERIALS AND METHODS

This study was conducted during the TONGA cruise (GEOTRACES GPpr14, doi:10.17600/18000884) between 1 November and 6 December 2019 (austral summer) onboard the *R/V L'Atalante*. Seawater samples were collected from two stations with contrasting biogeochemical conditions: station "volcano" (21.17°S, 175.93°E) with low phosphate and high iron concentrations; and station "gyre" (20.40°S, 166.59°W) with moderate phosphate and low iron concentrations (**Figure S1**).

### Experimental Setup

Seawater samples for DOP addition experiments were obtained from Niskin bottles mounted on a General Oceanics SBE911plus CTD profiler equipped with pressure, temperature, conductivity, and dissolved oxygen probes. Dissolved iron (DFe) concentrations were measured from samples collected using GoFlo bottles mounted on a trace metal clean rosette (Model 1018 Intelligent Rosette, General Oceanics).

Samples were collected from 7 to 9 m depth at the stations volcano and gyre, respectively, corresponding to a 50% photosynthetically active radiation (PAR) level. Seawater was distributed into fifteen 4.3-liter transparent polycarbonate bottles in five sets of triplicates. Three sets of triplicates were amended with adenosine monophosphate (AMP, with a P-monoester bond), adenosine triphosphate (ATP, with P-monoester and P-anhydride bonds) or sodium tripolyphosphate (3polyP, with P-anhydride bonds), respectively, to a final concentration of 20 µM P. Bottles were incubated for 48 h in on-deck incubators with running surface seawater and shaded with blue screening to mimic 50% PAR conditions. The two remaining triplicate bottle sets were kept unamended and treated as 'time zero' (immediately sampled at the beginning of the experiment) and 'control' (incubated for 48 h without any DOP amendment). All incubation bottles were sealed air-free with septum caps and spiked with nitrogen ($^{15}N_2$) stable isotopes for $N_2$ fixation measurements (see below).

Of each set of bottles, 1.5 L from two replicates were used for nucleic acid extractions, while 1.5 L of the third bottle was used for single-cell $N_2$ fixation measurements (see below). The remaining volume of each bottle was used to quantify dissolved nutrients, particulate organic carbon and nitrogen concentrations as well as for heterotrophic bacterial abundance and production rates (see below).

### Dissolved Nutrients and Particulate Organic Matter

Samples for the determination of dissolved iron (DFe) concentrations were collected according to GEOTRACES guidelines (www.geotraces.org/images/Cookbook.pdf) using a trace metal clean rosette attached to a 6 mm Kevlar cable. Seawater samples were filtered onboard (0.45 µm) using a polyethersulfone filter (Supor, Pall) and acidified within 24 h of collection with ultrapure hydrochloric acid (HCl, Merck, 0.2%, final pH 1.7). DFe was analyzed by flow injection analysis with chemiluminescence detection (Bonnet and Guieu, 2006).

Samples for nitrate plus nitrite ($NO_x$) and soluble reactive P (hereafter, phosphate) concentration were collected from Niskin bottles at each station cast and from each incubation bottle as described above. Sartoban® Cartridges were used to filter samples onboard through 0.2 µm and then stored at −20°C until analysis. Concentrations of all nutrients were determined using a segmented flow analyzer (AAIII HR, Seal Analytical)

according to Aminot and Kérouel (2009). Total dissolved P and nitrogen concentrations were analyzed using high-temperature (120°C) persulfate wet oxidation mineralization (Pujo-Pay and Raimbault, 1994). DOP and dissolved organic nitrogen concentrations were obtained by subtracting phosphate and NOx concentrations from the total dissolved P and nitrogen concentrations, respectively. The quantification limits were 0.05 µM for nitrate, 0.01 µM for nitrite, 0.5 µM for dissolved nitrogen, and 0.02 µM for phosphate and DOP.

Particulate nitrogen and carbon concentrations were determined using an elemental analyzer coupled to an isotope ratio mass spectrometer (EA-IRMS, INTEGRA 2, SerCon Ltd). After 48 h of incubation, 2.5 L of each set of triplicate incubation bottles was filtered onto pre-combusted (450°C, 4 h) glass fiber filters (GF/F, Whatman), dried at 60°C for 24 h, and stored at room temperature until analysis. Before analysis and after every ten samples, the instrument was calibrated using IAEA-600 reference material (caffeine), and the quantification limits were calculated as ten times the standard deviation of GF/F filter blank analyses. The quantification limit was ~5 µg for nitrogen and ~15 µg for carbon.

## Molecular Analyses

Seawater samples for nucleic acid extractions were filtered onto 0.2 µm polysulfone membrane filters (Supor, Pall), stored in sterile 2 ml bead beater tubes containing glass beads, and immediately flash-frozen in liquid nitrogen and stored at −80°C. In the lab, the filters were cut into two halves for DNA and RNA extraction, respectively. Filters were first ground and submitted to five to ten flash freezing steps with liquid nitrogen to maximize the extraction yield. DNA was then extracted using the DNeasy Blood & Tissue Kit (Qiagen Sciences, MD, USA) with a 4 h incubation for the proteinase K digestion step. RNA was extracted using the RNeasy Mini Kit (Qiagen Sciences, MD, USA) with β-mercaptoethanol (Sigma Aldrich, M6250) added to the lysis buffer RLT to enhance intracellular RNAse denaturation (Moisander et al., 2008). An extra DNAase treatment was performed using the TURBO DNA-free™ Kit (Ambion, Thermo Fisher Scientific), followed by a Zymo-5 column clean up kit (Zymo Research, USA). Nucleic acid concentrations were quantified using the PicoGreen dsDNA or RiboGreen RNA Quantification Kits (Invitrogen, Thermo Fisher Scientific) for DNA and RNA, respectively. To examine the expression of the nitrogenase gene *nifH*, first-strand complementary DNA (cDNA) was synthesized from RNA extracts using the TaqMan reverse transcription assay (Applied Biosystems, Life Technologies TM) following the procedure described by the manufacturer using the *nifH*3 reverse primer (Halm et al., 2009). Before the RNA retrotranscription, an outer *nifH* PCR was performed to check for residual DNA.

The abundance of *nifH* genes from the diazotrophs *Trichodesmium* and *Crocosphaera* was determined using Taqman (Life Technologies, Invitrogen) quantitative PCR (qPCR) assays as previously described (Church et al., 2005; Moisander et al., 2008). All assays were performed in a 12.5 µl reaction volume as follows: Taqman qPCR Master Mix (Applied Biosystems, Life Technologies), 1 pmol forward and reverse primers, 1 pmol probe, 0.1 µg $\mu L^{-1}$ BSA, and 1–3 ng DNA or cDNA template per reaction. Thermal conditions were 2 min at 50°C, 10 min at 95°C, and 45 cycles of 30 min 95°C, 1 min 60°C. Eight 10-fold dilutions of the standard were included in each run. Standards were generated from custom-produced plasmids with the target insert of interest (GENEWIZ Co. Ltd., Suzhou, China). Plasmids were linearized by HindIII digestion (Thermo Fisher Scientific), gel purified, and quantified using Picogreen. Inhibition tests were performed for all environmental samples using a concentration standard of 800 gene copies $\mu l^{-1}$. All standards were run in duplicates, samples were run in triplicates, and two no-template controls were included in each run. The limit of detection (LOD) and detectable but unquantifiable (DNQ) limits in these assays were 1 and 8 gene copies per reaction, respectively, corresponding to an average of 60 *nifH* gene copies $L^{-1}$ (LOD) and 477 *nifH* gene copies $L^{-1}$ (DNQ). Amplification below LOD was defined as 0 copies, whereas *nifH* amplification above LOD but below DNQ was assigned a conservative value of one *nifH* gene copy $L^{-1}$. Thirty of 80 samples were quantified by duplicate measurements when one of the triplicates failed to amplify, and knowing that the successful samples were above the DNQ threshold.

## Cell Specific $N_2$ Fixation Rates

The $^{15}N/^{14}N$ ratio of single *Trichodesmium* filaments and *Crocosphaera* cells was analyzed by nanoscale secondary ion mass spectrometry using a NanoSIMS 50L (Cameca, Gennevilliers, France) at the Leibniz Institute for Baltic Sea Research (IOW, Germany). A volume of 1.5 L from one replicate of each treatment was filtered onto a 1 µm polycarbonate filter and fixed with 1.6% paraformaldehyde prepared with 0.2 µm filtered SW to avoid cell exudation and potential losses of the tracers. After epifluorescence inspection of all samples, several sections of each filter were mounted once dried with conductive tape on 10 × 5 mm aluminum stubs (Ted Pella) and gold-coated to a thickness of ca. 30 nm (Cressington 108 auto sputter coater). A 1 pA 16 keV Cesium ($Cs^+$) primary beam was scanned on a 512 × 512 pixel raster with a raster area of 15 × 15 µm and a counting time of 250 µs per pixel. Before analyses, samples were pre-sputtered with 600 pA $Cs^+$ current for 2 min in a raster of 30 × 30 µm to remove the gold and surface contaminants and reach the steady state of ion formation. Negative secondary ions $^{12}C$–, $^{13}C$–, $^{12}C^{14}N$–, $^{12}C^{15}N$– and $^{31}P$– were detected with electron multiplier detectors (Hamamatsu), and secondary electrons were simultaneously imaged. Sixty serial quantitative secondary ion mass planes were generated, drift corrected, and accumulated to the final image. The mass resolving power was >8,000 (Cameca's definition) in order to resolve isobaric interferences. Data were processed using the Look@nanoSIMS software (Polerecky et al., 2012). Isotope ratio images were generated by dividing the ion counts of $^{12}C^{15}N$- by $^{12}C^{14}N$- pixel by pixel. *Trichodesmium* filaments and *Crocosphaera* cells were identified in nanoSIMS secondary electron $^{12}C$-,$^{12}C^{14}N$- and $^{31}P$- images, which were used to define the regions of interest (ROIs). For each ROI, the $^{15}N/(^{14}N+^{15}N)$ ratios were calculated based on the ion counts averaged over the ROIs. Because *Trichodesmium* and *Crocosphaera* have strikingly

different sizes and biomasses, we preferred to compute biomass-independent cell-specific $N_2$ fixation rates as follows:

$$\text{Cell} - \text{specific } N_2 \text{fixation} = \frac{A_{cell} - A_{Nat}}{A_{N_2} - A_{Nat}} \times \frac{1}{t}$$

where $A_{cell}$ is the $^{15}N$ atom % enrichment of individual *Trichodesmium* or *Crocosphaera* cells, $A_{Nat}$ is the natural $^{15}N$ atom % enrichment measured in cells at time zero, $A_{N2}$ is the $^{15}N$ atom % enrichment of dissolved $N_2$ in seawater and *t* is the incubation time. The rates obtained have units of $d^{-1}$.

## Heterotrophic Bacteria Abundance and Production Rates

Heterotrophic bacteria (HB) were enumerated by flow cytometry. From all incubation treatments, 1.8 ml was subsampled from each triplicate 4.3 L bottle into cryotubes, fixed with paraformaldehyde (200 µl, 4% final concentration) for 5 min at room temperature, flash-frozen in liquid nitrogen, and stored at −80°C until analysis. Back in the lab, all samples were thawed, cells stained with 2 µL SYBR Green I at 1/10× of the stock solution (10,000×, Invitrogen, Life Technologies, Thermo Fisher Scientific, France) and measured using a CytoFLEX flow cytometer (Beckman Coulter) fitted with violet (405 nm), blue (488 nm), and red (638 nm) lasers. Trucount TM beads (BD Biosciences) were used to determine the volume analyzed, and fluoresbrite 2 µm latex beads (Polysciences, Inc., Warrington, PA, United States) were also added as internal size standards to all samples before analysis. Samples were run at low speed (10–30 µl $min^{-1}$) and HB was identified in a plot of side scatter (SSC) versus green fluorescence (FL1).

Bacterial production was determined onboard using $^3H$–leucine incorporation (Kirchman, 2018) and microcentrifugation (Smith and Azam, 1992) as detailed in Van Wambeke et al. (2018). Briefly, triplicate 1.5 ml samples and a control killed with trichloroacetic acid (TCA; 5% final concentration) were incubated with a mixture of [4,5-$^3H$]-leucine (Perkin-Elmer, specific activity 100 Ci $mmol^{-1}$) and nonradioactive leucine at final concentrations of 14 and 7 nM, respectively. Samples were incubated in the dark at the respective *in situ* temperatures for 1–2 h. A factor of 1.5 kg C mol $leucine^{-1}$ was used to convert leucine incorporation into carbon. Standard deviations from triplicate measurements averaged 7%.

## Statistical Analyses

The integrated development environment for the statistical software R, RStudio (RRID: SCR_000432, Version 1.3.1093), was used to process and analyze data and produce graphs. All differences between treatments, species, or stations for all parameters and other statistical patterns were evaluated by one-way ANOVA, after checking data for normality and heterogeneity of variance (QQ plot, Shapiro–Wilk test, and *Levene's* test). For the *post hoc* analysis, the Tukey HSD test was used to determine pairwise differences between groups. The Dunnett's test was performed when comparing the average responses of all DOP treatments to the control. A paired Students' *t*-test was applied when comparing average responses to a specific treatment between stations. Pearson correlations are used to examine the potential coupling or relationship between certain variables. Statistical significance for all tests was set for p-values lower than 0.05 (95% confidence level).

# RESULTS

## Biogeochemical Conditions

Phosphate concentrations in the upper 50 m (mixed layer depth) of the volcano station were equal to or below the quantification limit and lower than those at the gyre station (0.07 µM P; **Figure S2A**). In contrast, DFe concentrations within the same depth range (0.15–0.87 nM) were more than five times higher at the volcano than at the gyre station (Tilliette et al., 2022; *t*-test, p = 0.07, n = 3; **Figure S2B**). Temperature was similar between stations (**Figure S2C**) and salinity and dissolved oxygen concentrations were slightly lower at the volcano than at the gyre station (*t*-test, p<0.1, n = 3; **Figures S2D, E**). Conversely, chlorophyll-*a* in the upper 50 m showed higher concentrations at the volcano than at the gyre station (*t*-test, p = 0.02, n = 4), where a deep chlorophyll maximum was observed below 100 m (**Figure S2F**).

The initial (time zero) average phosphate concentrations in the incubation bottles were 3.4 lower at the volcano than at the gyre experiment (*t*-test, p<0.001; **Table S1**). Dissolved organic phosphorous and nitrogen concentrations were similar at both stations (0.18–0.21 µM P and 6.4–6.2 µM N), whereas $NO_x$ concentrations were twice high at the volcano (0.08 µM) than at the gyre station (0.04 µM, *t*-test, p = 0.06; **Table S1**).

## *Trichodesmium* and *Crocosphaera In Situ* and in Treatments

At the beginning of our experiments (initial conditions), *Trichodesmium* was dominant at the volcano station ($6.2 \times 10^5$ *nifH* copies $L^{-1}$) but less abundant at the gyre, where around three filaments were observed ($2.8 \times 10^4$ *nifH* copies $L^{-1}$; **Figures 1A, B**), whereas *Crocosphaera* was abundant at both stations ($1.8–2.4 \times 10^4$ *nifH* copies $L^{-1}$; **Figures 1D, E**). *Trichodesmium nifH* transcripts were approximately 4,000 times higher at the volcano than at the gyre station, but due to the variability between experimental duplicates, this difference was not significant (*t*-test, p = 0.243; **Figure 1C**). Conversely, *Crocosphaera nifH* transcripts were 28 times lower at the volcano than at the gyre station (*t*-test, p = 0.197; **Figure 1F**).

In DOP-amended incubations at the volcano station, the abundance of *Trichodesmium nifH* genes decreased by one order of magnitude relative to the control after 48 h, which was particularly pronounced in the ATP treatment (~4 times lower; Dunnett's test, p = 0.065, **Figure 2A**). At the gyre station, *Trichodesmium nifH* genes were significantly higher in the AMP treatment than in the control (Dunnett's test, p<0.001, **Figure 2B**) but not when compared with the time zero samples (**Figure 1**). The expression of *nifH* in *Trichodesmium* was similar or lower than the control in all DOP incubations for both experiments

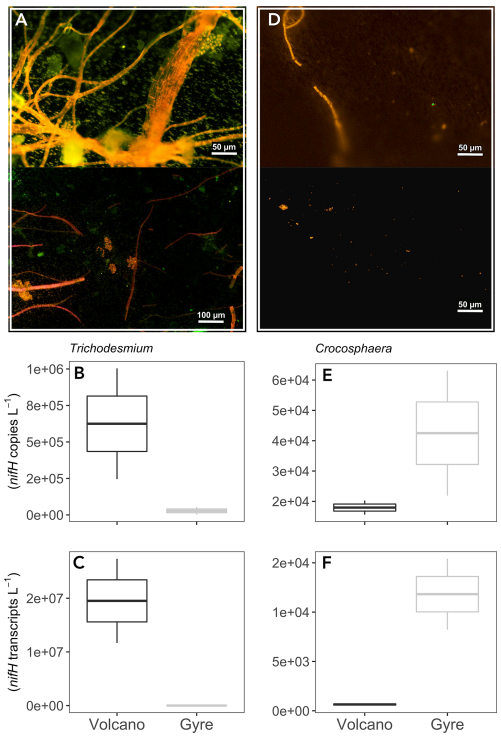


**FIGURE 1 |** Epifluorescence microscopy images from the time zero samples inspected before NanoSIMS analysis showing main diazotrophic communities at the volcano **(A)** and at the gyre station **(D)**. Boxplots represent average *nifH* abundances and transcripts of *Trichodesmium* **(B, C)** and *Crocosphaera* **(E, F)** from duplicate time zero samples measured by qPCR in triplicate at each station.

(**Figures 2C, D**). *Crocosphaera nifH* copies were ~three times lower at the volcano than at the gyre (*t*-test, p = 0.011, **Figures 2E, F**) and did not vary significantly in response to any DOP addition at any of the two stations (Dunnett's Test, p>0.8). However, *Crocosphaera nifH* expression increased in the AMP and 3polyP treatments at the volcano station, yet this response was not significant (Dunnett's Test, p = 0.17, **Figure 2G**). Instead, *Crocosphaera nifH* expression increased significantly in the AMP treatment at the gyre (Dunnett's Test, p = 0.0014, **Figure 2H**).

## Single-Cell $N_2$ Fixation Rates Change in Response to DOP Additions

We present single-cell $N_2$ fixation rates as biomass-independent rates (here called "cell-specific" rates in $d^{-1}$; see *Materials and Methods*). This allows a better comparison of the response of *Trichodesmium* and *Crocosphaera* to DOP additions than using bulk $N_2$ fixation rates as both diazotrophs differ in biomass and abundance. At the volcano station, *Trichodesmium* cell-specific $N_2$ fixation rates were not significantly different between the control and all the DOP treatments (Dunnett's Test, p >0.2; **Figure 3A**). Still, the lowest rates were measured in the ATP treatment (**Figure 3A**). At the gyre station, the abundance of *Trichodesmium* was low (**Figures 1**, **2B**), and only a few cell-specific $N_2$ fixation rate measurements could be done from the AMP and control treatments, which showed equally low values (*t*-test, p = 0.81; **Figure 3B**). At the volcano station, *Crocosphaera* cell-specific $N_2$ fixation was stimulated by AMP (Dunnett's Test, p<0.001) and 3polyP (**Figure 3C**). At the gyre station, *Crocosphaera* cell-specific $N_2$ fixation rates were ~100 times lower than those at the volcano (*t*-test, p<0.001; compare **Figures 3C, D**) and doubled in the 3polyP treatment compared to the control (Dunnett's Test, p<0.001, **Figure 3D**). No *Crocosphaera* cells were identified for cell-specific nanoSIMS analyses in ATP treatment samples at any station.

## Response of Heterotrophic Bacteria to DOP Additions

Over the incubation period at both stations, the abundance of HB increased >five times in the ATP treatment compared to the control (Dunnett's Test, p<0.002; **Figures 4A, B**). In the 3polyP treatment, HB abundances were also elevated compared with the controls at both stations; however, these changes were not significant (Dunnett's Test, p >0.3; **Figures 4A, B**).

HB production rates followed the same pattern as the abundance of HB, increasing in the ATP and 3polyP treatments with respect to the controls at both stations (**Figures 4C, D**), but was only significant at the volcano station (Dunnett's Test, p<0.01). Interestingly, the increase in particulate nitrogen in the ATP treatments observed at both stations coincided with the highest HB activity (4.3–5.8 µM, **Table S1**, Dunnett's Test, p<0.01). Additionally, particulate organic carbon reached similar concentrations at both stations in the ATP treatment (**Table S1**).

# DISCUSSION

*Trichodesmium* and *Crocosphaera* are widespread cyanobacterial diazotrophs that are commonly limited by P availability in the global ocean (Dyhrman et al., 2007). Under phosphate limiting conditions, *Trichodesmium* can exploit P-esters (P–O–C bond) or reduced P molecules such as phosphonates (P–C bond) (Dyhrman et al., 2002; Orchard et al., 2003), while *Crocosphaera* can only use P-esters (Dyhrman and Haley, 2006). Here we explored the potential of P-anhydrides compared to P-esters as a resource for diazotrophs under contrasting phosphate availability.

At the volcano station, *Trichodesmium* was abundant (**Figures 1**, **2**) but did not significantly respond to any DOP treatment tested (**Figures 3A, C**). This suggests that *Trichodesmium* was not limited by P at this station, despite the low phosphate concentrations measured (**Figure S2**, **Table S1**). Previous research showed that phosphate turnover times in this region vary by two orders of magnitude, indicating a highly dynamic cycling of P induced by intense microbial activity and by the (sub)mesoscale variability in surface circulation (Van Wambeke et al., 2018; Rousselet et al., 2018). Such active P cycling has been observed in other subtropical gyre regions (Corno et al., 2007; Calil and Richards, 2010; Björkman et al., 2012). The success of *Trichodesmium* in these regions lies in its ability to maintain stable levels of P uptake in spite of variable

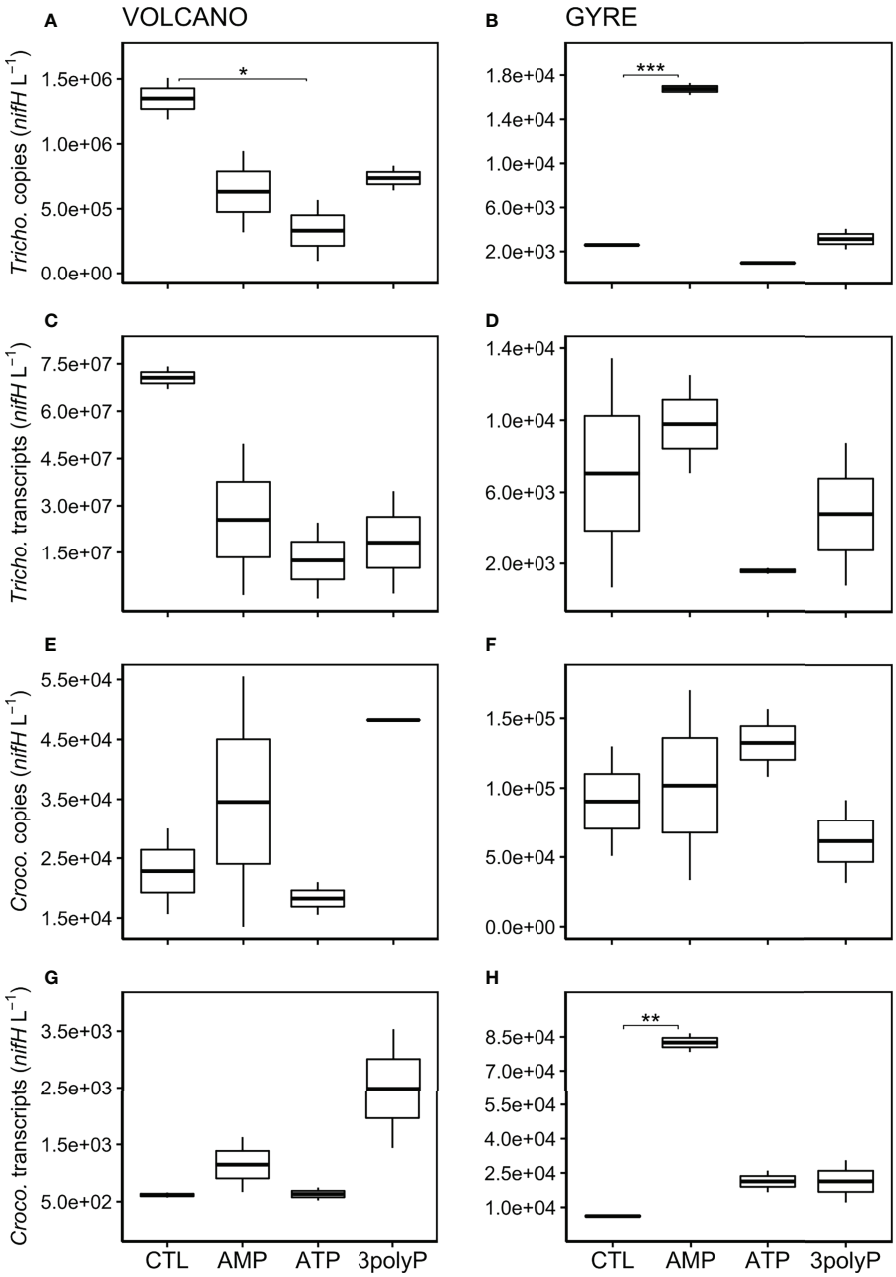


**FIGURE 2 |** Abundance of *Trichodesmium* and *Crocosphaera nifH* copies and transcripts after incubations. Boxplots represent averaged *nifH* copies (DNA) and transcripts (cDNA) abundances ($L^{-1}$) from qPCR measurements in triplicate from each treatment duplicate for *Trichodesmium* at the volcano **(A, C)** and at the gyre station **(B, D)**, and *Crocosphaera* at the volcano **(E, G)** and at the gyre station **(F, H)**, respectively. Significant differences in *nifH* copies or transcripts between the control and the DOP treatments were tested with the Dunnett's Test and represented by the horizontal lines with significant codes (***p<0.001, **p<0.01, *p<0.1).

P conditions (Fu et al., 2005; Orchard et al., 2010a; Frischkorn et al., 2018). Instead, the low DFe conditions of the gyre are thought to inhibit the growth of *Trichodesmium* despite the non-limiting phosphate concentrations (Halm et al., 2011; Moisander et al., 2012; Stenegren et al., 2018), whereas *Crocosphaera* is shown to be better adapted to such conditions (Küpper et al., 2008; Saito et al., 2011; Benavides et al., 2022; Lory et al., 2022).

*Crocosphaera* $N_2$ fixation rates responded to AMP at the volcano station and to 3polyP at both stations (**Figures 3C, D**). The higher phosphate concentrations measured in the 3polyP as compared to the AMP treatment at the volcano station (**Table S1**) suggested that 3polyP was mainly hydrolyzed by *Crocosphaera* and HB to acquire P and likely also energy. In turn, the increase in $N_2$ fixation by *Crocosphaera* in the AMP treatment at the volcano indicates they were P-limited and therefore had to hydrolize AMP to obtain P, as observed in previous studies where similar P-ester molecules served as a sole P source for *Crocosphaera* (Dyhrman and Haley, 2006). Still, despite the important release

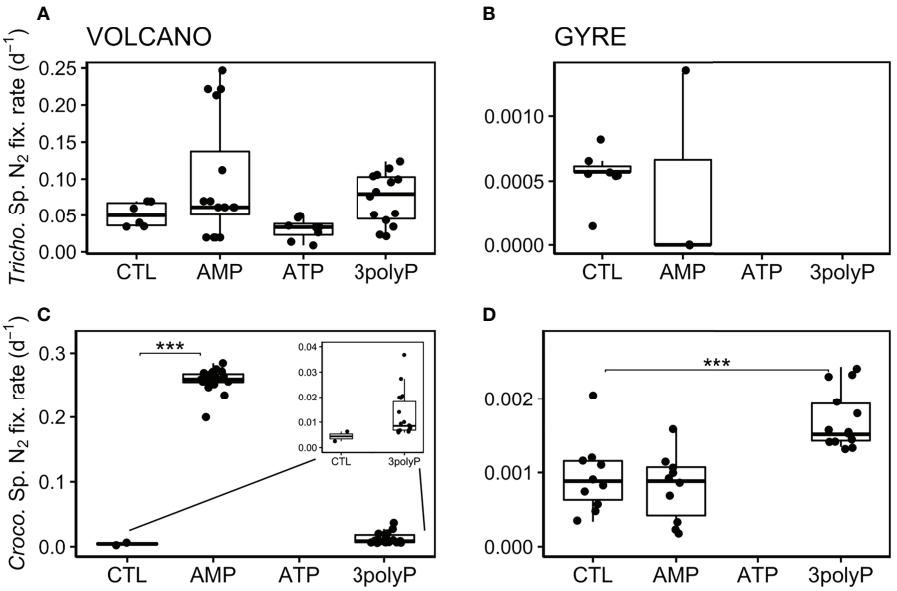


**FIGURE 3 |** Biomass-independent cell-specific $N_2$ fixation rates. Boxplots represent averaged cell-specific $N_2$ fixation rates derived from NanoSIMS per-cell enrichments over the experimental incubations. Each data point represents a single *Crocosphaera* and one or several averaged *Trichodesmium*'s cell measurement as they showed similar enrichment values along the trichomes. No data is shown when cells were not found or identified. Significant differences in the cell-specific rates between the control and the DOP treatments were tested with the Dunnett's Test and represented by the horizontal lines with significance codes (***p<0.001).

of phosphate and the potential energy acquisition during the degradation of 3polyP, *Crocosphaera* $N_2$ fixation responses did not show an additive effect as compared to the AMP treatment. The released phosphate was in excess of the growth requirements of *Crocosphaera* (considering a P:C ratio of 0.007 (Inomura et al., 2019) and a carbon cell content of 8.77 pg C cell$^{-1}$ (Lory et al., 2022). Therefore, even if *Crocosphaera* populations from the volcano station were P-limited and benefited from phosphate either directly or indirectly released from 3polyP, we would not expect these cells to take up all the phosphate released over the incubation period. Moreover, in the 3polyP treatment, HB highly developed and presented significantly higher production rates as

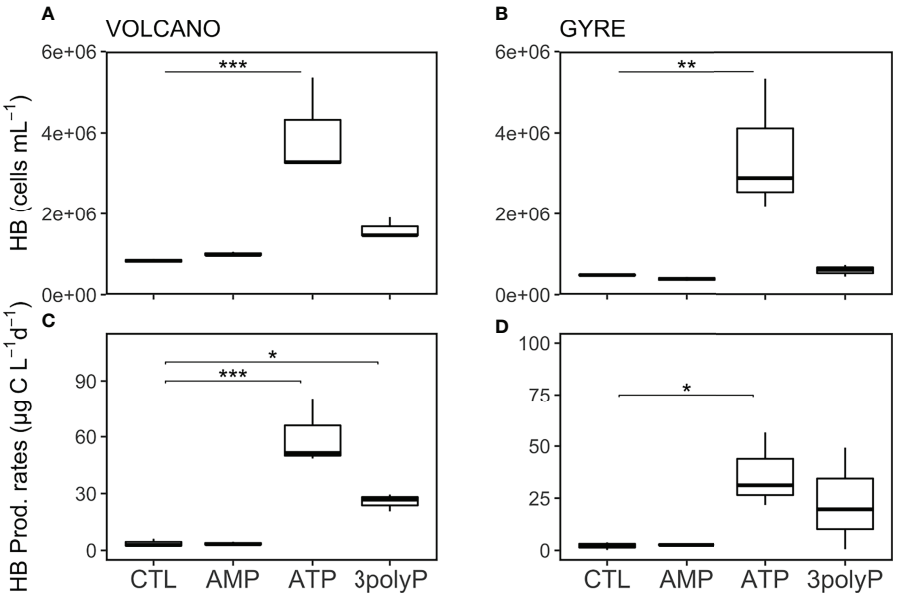


**FIGURE 4 |** Abundance and production rates of heterotrophic bacteria. Boxplots represent averaged heterotrophic bacteria (HB) abundance **(A, B)** and production rates **(C, D)** from each treatment triplicate at the volcano and the gyre station, respectively. Significant differences in cell abundance between the control and the DOP treatments were tested with the Dunnett's Test and represented by the horizontal lines with significance codes (***p<0.001, **p<0.01, *p<0.1).

compared to the AMP and control treatments, likely increasing the competition for other resources which might have limited $N_2$ fixation in *Crocosphaera*. Still, in terms of growth (*nifH* copies) and *nifH* expression (*nifH* transcripts), *Crocosphaera* showed a positive effect when 3polyP was added as compared to AMP, where the responses were more variable, possibly reflecting an alternative way they might use the energy from 3polyP (**Figures 2E, G**). While P-esters are well documented as a source of P for *Crocosphaera* (Dyhrman and Haley, 2006), the use of 3polyP has not been observed before. Previous studies have shown that key marine microbes such as *Synechococcus* and *Prochlorococcus* (Moore et al., 2005), the coccolithophore *Emiliania huxleyi*, several *Thalassiosira* spp. diatoms (Diaz et al., 2016; Diaz et al., 2018; Diaz et al., 2019), and the heterotrophic bacterium *Ruegeria pomeroyi* (Adams et al., 2022) can grow on 3polyP as the sole P source. Here we propose that 3polyP can be utilized for both P and energy acquisition, but also that microbial interactions such as competition might control the specific exploitation of distinct DOP, reinforcing the currently accepted level of complexity of the P cycle (Duhamel et al., 2021).

The enhanced $N_2$ fixation rates of *Crocosphaera* in 3polyP treatments at the gyre station were not mirrored by an increase in their *nifH* gene copies (**Figure 2F**). This suggests that 3polyP was used as a source of energy to fuel the expensive process of $N_2$ fixation rather than as a source of P for growth in these phosphate-rich waters. Indeed, 3polyP has been described as the primitive energy donor in the origin of life and therefore the precursor of ATP (Kornberg, 1995; Lipmann, 1965). Cyanobacteria of the genus *Nostoc* have shown the ability to use strictly intracellular polyP as an alternative source of energy-rich phosphate to phosphorylate glucose by the action of a glucokinase enzyme (Albi and Serrano, 2015). Moreover, a mechanism that enables some mammalian cells to extracellularly transform the energy stored in polyP bonds into metabolic energy in the form of ATP has been described (Müller et al., 2019). The mechanism involves the concerted enzymatic action of the alkaline phosphatase and adenylate kinase, which consecutively work to channel the energy from polyP to a final energy-consumption step where ATP is produced (Müller et al., 2019). A similar combination of enzymes may operate in *Crocosphaera* to obtain energy from 3polyP.

Surprisingly, *Trichodesmium* did not seem to benefit from the more readily available ATP and we could not assess the ATP usage by *Crocosphaera* as no cells were found during nanoSIMS analysis in this treatment; **Figures 2**, **3**). This was unexpected since ATP can provide up to 25% of the total P uptake by *Trichodesmium* in the oligotrophic Sargasso Sea (Orchard et al., 2010a). The increase in HB abundance and production rates in ATP incubation (**Figure 4**) suggests that HB was more competitive for ATP than diazotrophs, as previously observed (Michelou et al., 2011). Along the same lines, Björkman and co-authors found that despite HB and *Prochlorococcus* being equal competitors for phosphate in the North Pacific, HB is more effective at scavenging ATP (Björkman et al., 2012). In the South Pacific, (Van Wambeke et al. 2008, 2018) found that HB were mainly limited by the availability of energy or labile carbon, as glucose additions stimulated HB production rates to a larger extent than phosphate or nitrogen (Van Wambeke et al. 2008, 2018). ATP molecules contain three atoms of P, five atoms of nitrogen, 10 atoms of carbon and several hydrogen and oxygen atoms. Hence, besides being a source of energy, we speculate that HB may hydrolyze ATP to acquire nitrogen and carbon to sustain growth (Wilkins, 1972; Wanner and McSharry, 1982; Hoppe and Ullrich, 1999). This idea is supported by the increase in non-labelled particulate nitrogen and organic carbon concentrations observed in ATP treatments (**Table S1**).

In contrast with previous studies indicating that 3polyP can be a source of P for marine microbes (Moore et al., 2005; Diaz et al., 2016; Diaz et al., 2018; Diaz et al., 2019), our results indicate that diazotrophs may rely on other DOP compounds as nutritional P resources, such as P-esters and phosphonates (Dyhrman and Haley, 2006). However, the environmental conditions of our study were not severely P-limited, hindering our ability to comprehensively assess the potential of 3polyP as an alternative P source for diazotrophs. Notwithstanding, polyP compounds represent an important fraction of the marine DOP pool (Young and Ingall, 2010) and may serve as an alternative source of energy for diazotrophs to sustain the expensive process of N2 fixation. In the increasingly stratified and nutrient-poor future oceans, diazotroph-derived nitrogen inputs may rely on energy-rich compounds such as P-anhydrides.

## DATA AVAILABILITY STATEMENT

The original contributions presented in the study are included in the article/**Supplementary Material**. Further inquiries can be directed to the corresponding author.

## AUTHOR CONTRIBUTIONS

MB, SD, JD, FW, and EP-V conceived and designed the experiment. MB, FW, and EP-V performed the experiment at sea. AF analyzed the samples and the data with support from AV for NanoSIMS analysis. AF wrote the manuscript with input from all co-authors. All authors contributed to the article and approved the submitted version.

## FUNDING

This research was supported by the NOTION BNP Paribas Foundation for Climate and Biodiversity (MB and LR) the TONGA project (Shallow hydroThermal sOurces of trace elemeNts: potential impacts on biological productivity and the bioloGicAl carbon pump; TONGA cruise DOI: 10.17600/18000884) funded by the Agence Nationale de la Recherche (grant TONGA ANR-18- CE01-0016 and grant CINNAMON ANR-17-CE2-0014-01), the LEFE-CyBER program (CNRS-INSU), the A-Midex foundation, the Institut de Recherche pour le Développement (IRD). The MIMS equipment used in this study was obtained with European FEDER Funds. The NanoSIMS at the Leibnitz-Institute for Baltic Sea research in Warnemuende (IOW) was

funded by the German Federal Ministry of Education and Research (BMBF), grant identifier 03F0626A.

## ACKNOWLEDGMENTS

The authors would like to thank the captain and crew of *R/V L'Atalante*. We are indebted to S. Hallstrøm, L. W. von Friesen, and M. Bittner for their assistance with molecular analyses, and to S. Helias-Nunige for assistance with inorganic and organic nutrient analyses. Annett Grüttmüller is acknowledged for NanoSIMS routine operation.

## SUPPLEMENTARY MATERIAL

The Supplementary Material for this article can be found online at: https://www.frontiersin.org/articles/10.3389/fmars.2022.923765/full#supplementary-material

## REFERENCES

Adams, J. C., Steffen, R., Chou, C., Duhamel, S. and Diaz, J. M. (2022). Dissolved Organic Phosphorus Utilization by the Marine Bacterium Ruegeria Pomeroyi DSS-3 Reveals Chain Length-Dependent Polyphosphate Degradation. *Environ. Microbiol.* 24 (5), 2259–2269. doi: 10.1111/1462-2920.15877

Albi, T. and Serrano, A. (2015). Two Strictly Polyphosphate-Dependent Gluco(Manno)Kinases From Diazotrophic Cyanobacteria With Potential to Phosphorylate Hexoses From Polyphosphates. *Appl. Microbiol. Biotechnol.* 99, 3887–3900. doi: 10.1007/s00253-014-6184-7

Aminot, A., Kérouel, R., and Coverly, S. C. (2009). Nutrients in Seawater Using Segmented Flow Analysis. *In Practical Guidelines for the Analysis of Seawater.* 155–190. do: 10.1201/9781420073072

Benavides M., Caffin M., Duhamel S., Foster R. A., Grosso O., Guieu C., Van Wambeke F., Bonnet S. (2022). Anomalously High Abundance of Crocosphaera in the South Pacific Gyre. *FEMS Microbiol Lett.* 369 (1), fnac039. doi: 10.1093/femsle/fnac039

Björkman, K., Duhame, S. and Kar, D. M. (2012). Microbial Group Specific Uptake Kinetics of Inorganic Phosphate and Adenosine-5′-Triphosphate (ATP) in the North Pacific Subtropical Gyre. *Front. Microbiol.* 3. doi: 10.3389/fmicb.2012.00189

Björkman, K. and Karl, D. M. (1994). Bioavailability of Inorganic and Organic Phosphorus Compounds to Natural Assemblages of Microorganisms in Hawaiian Coastal Waters. *Mar. Ecol. Prog. Ser.* 111, 265–273. doi: 10.3354/meps111265

Bonnet, S. and Guieu, C. (2006). Atmospheric Forcing on the Annual Iron Cycle in the Western Mediterranean Sea: A 1-Year Survey. *J. Geophys. Res. Ocean.* 111(C09010). doi: 10.1029/2005JC003213

Calil, P. H. R. and Richards, K. J. (2010). Transient Upwelling Hot Spots in the Oligotrophic North Pacific. *J. Geophys. Res. Ocean.* 115 (C2). doi: 10.1029/2009JC005360

Church, M. J., Jenkins, B. D., Karl, D. M. and Zehr, J. P. (2005). Vertical Distributions of Nitrogen-Fixing Phylotypes at Stn ALOHA in the Oligotrophic North Pacific Ocean. *Aquat. Microb. Ecol.* 38, 3–14. doi: 10.3354/ame038003

Corno, G., Karl, D. M., Church, M. J., Letelier, R. M., Lukas, R., Bidigare, R. R., et al. (2007). Impact of Climate Forcing on Ecosystem Processes in the North Pacific Subtropical Gyre. *J. Geophys. Res. Ocean.* 112 (C04021). doi: 10.1029/2006JC003730

Diaz, J. M., Björkman, K. M., Haley, S. T., Ingall, E. D., Karl, D. M., Longo, A. F., et al. (2016). Polyphosphate Dynamics at Station ALOHA, North Pacific Subtropical Gyre. *Limnol. Oceanogr.* 61, 227–239. doi: 10.1002/lno.10206

Diaz, J. M., Holland, A., Sanders, J. G., Bulski, K., Mollett, D., Chou, C. W., et al. (2018). Dissolved Organic Phosphorus Utilization by Phytoplankton Reveals Preferential Degradation of Polyphosphates Over Phosphomonoesters. *Front. Mar. Sci.* 5. doi: 10.3389/fmars.2018.00380

Diaz, J. M., Steffen, R., Sanders, J. G., Tang, Y. and Duhamel, S. (2019). Preferential Utilization of Inorganic Polyphosphate Over Other Bioavailable Phosphorus Sources by the Model Diatoms Thalassiosira Spp. *Environ. Microbiol.* 21, 2415–2425. doi: 10.1111/1462-2920.14630

Duhamel, S., Diaz, J. M., Adams, J. C., Djaoudi, K., Steck, V. and Waggoner, E. M. (2021). Phosphorus as an Integral Component of Global Marine Biogeochemistry. *Nat. Geosci.* 14, 359–368. doi: 10.1038/s41561-021-00755-8

Dyhrman, S. T., Ammerman, J. W. and van Mooy, B. A. S. (2007). Microbes and the Marine Phosphorus Cycle. *Oceanography* 20, 110–116. doi: 10.5670/oceanog.2007.54

Dyhrman, S. T., Chappell, P. D., Haley, S. T., Moffett, J. W., Orchard, E. D., Waterbury, J. B., et al. (2006). Phosphonate Utilization by the Globally Important Marine Diazotroph Trichodesmium. *Nature* 439, 68–71. doi: 10.1038/nature04203

Dyhrman, S. T. and Haley, S. T. (2006). Phosphorus Scavenging in the Unicellular Marine Diazotroph Crocosphaera Watsonii. *Appl. Environ. Microbiol.* 72, 1452–1458. doi: 10.1128/AEM.72.2.1452-1458.2006

Dyhrman, S. T., Webb, E. A., Anderson, D. M., Moffett, J. W. and Waterbury, J. B. (2002). Cell-Specific Detection of Phosphorus Stress in Trichodesmium From the Western North Atlantic. *Limnol. Oceanogr.* 47, 1832–1836. doi: 10.4319/lo.2002.47.6.1832

Falkowski, P. (2001). "Biogeochemical Cycles," in *Encyclopedia of Biodiversity: Second Edition*, vol. 552–564. (Elsevier Inc). doi: 10.1016/B978-0-12-384719-5.00013-7

Frischkorn, K. R., Krupke, A., Guieu, C., Louis, J., Rouco, M., Salazar Estrada, A. E., et al. (2018). Trichodesmium Physiological Ecology and Phosphate Reduction in the Western Tropical South Pacific. *Biogeosciences* 15, 5761–5778. doi: 10.5194/bg-15-5761-2018

Fu, F., Zhang, Y., Bell, P. R. F. and Hutchins, D. A. (2005). Phosphate Uptake And Growth Kinetics Of Trichodesmium (Cyanobacteria) Isolates From The North Atlantic Ocean And The Great Barrier Reef, Australia 1. *J. Phycol.* 41, 62–73. doi: 10.1111/j.1529-8817.2005.04063.x

Halm, H., Lam, P., Ferdelman, T. G., Lavik, G., Dittmar, T., Laroche, J., et al. (2011). Heterotrophic Organisms Dominate Nitrogen Fixation in the South Pacific Gyre. *ISME. J.* 6, 1238–1249. doi: 10.1038/ismej.2011.182

Halm, H., Musat, N., Lam, P., Langlois, R., Musat, F., Peduzzi, S., et al. (2009). Co-Occurrence of Denitrification and Nitrogen Fixation in a Meromictic Lake, Lake Cadagno (Switzerland). *Environ. Microbiol.* 11, 1945–1958. doi: 10.1111/j.1462-2920.2009.01917.x

Hoppe, H.-G. and Ullrich, S. (1999). Profiles of Ectoenzymes in the Indian Ocean: Phenomena of Phosphatase Activity in the Mesopelagic Zone. *Aquat. Microb. Ecol.* 19, 139–148. doi: 10.3354/ame019139

Inomura, K., Masuda, T. and Gauglitz, J. M. (2019). Active Nitrogen Fixation by Crocosphaera Expands Their Niche Despite the Presence of Ammonium – A Case Study. *Sci. Rep.* 9, 1–11. doi: 10.1038/s41598-019-51378-4

Karl, D. M. (2000). Phosphorus, the Staff of Life. *Nature.* 406, 31–33.

Karl, D. M. (2014). Microbially Mediated Transformations of Phosphorus in the Sea: New Views of an Old Cycle. *Ann. Rev. Mar. Sci.* 6, 279–337. doi: 10.1146/annurev-marine-010213-135046

Karl, D. M. and Björkman, K. M. (2015). "Dynamics of Dissolved Organic Phosphorus," in *Biogeochemistry of Marine Dissolved Organic Matter* (Elsevier), 233–334. doi: 10.1016/B978-0-12-405940-5.00005-4

Kemena, T. P., Landolfi, A., Oschlies, A., Wallmann, K. and Dale, A. W. (2019). Ocean Phosphorus Inventory: Large Uncertainties in Future Projections on Millennial Timescales and Their Consequences for Ocean Deoxygenation. *Earth Syst. Dyn.* 10, 539–553. doi: 10.5194/esd-10-539-2019

Kirchman, D. L. (2018). "Leucine Incorporation as a Measure of Biomass Production by Heterotrophic Bacteria," in *Handbook of Methods in Aquatic Microbial Ecology* (CRC Press), 509–512. doi: 10.1201/9780203752746

Kornberg, A. (1995). Inorganic Polyphosphate: Toward Making a Forgotten Polymer Unforgettable. *J. Bacteriol.* 177, 491–496. doi: 10.1128/jb.177.3.491-496.1995

Küpper, H., Šetlík, I., Seibert, S., Prášil, O., Šetlikova, E., Strittmatter, M., et al. (2008). Iron Limitation in the Marine Cyanobacterium Trichodesmium Reveals New Insights Into Regulation of Photosynthesis and Nitrogen Fixation. *New Phytol.* 179, 784–798. doi: 10.1111/j.1469-8137.2008.02497.x

Li, J. and Dittrich, M. (2019). Dynamic Polyphosphate Metabolism in Cyanobacteria Responding to Phosphorus Availability. *Environ. Microbiol.* 21, 572–583. doi: 10.1111/1462-2920.14488

Lipmann, F. (1965). "Projecting Backward From the Present Stage of Evolution of Biosynthesis," in *The Origin of Prebiological Systems and of their Molecular Matrices, ed. S. W. Fox* (New York, NY: Academic Press), 259–280.

Lory, C., Van Wambeke, F., Fourquez, M., Berman-Frank, I., Barani, A., Tilliette, C., et al. (2022). Assessing the Contribution of Diazotrophs to Microbial Fe Uptake Using a Group Specific Approach in the Western Tropical South Pacific Ocean. *ISME. COMMUN. J.* 2, 41. doi: 10.1038/s43705-022-00122-7

Martin, P., Dyhrman, S. T., Lomas, M. W., Poulton, N. J. and Van Mooy, B. A. S. (2014). Accumulation and Enhanced Cycling of Polyphosphate by Sargasso Sea Plankton in Response to Low Phosphorus. *Proc. Natl. Acad. Sci. U. S. A.* 111, 8089–8094. doi: 10.1073/pnas.1321719111

Michelou, V. K., Lomas, M. W. and Kirchman, D. L. (2011). Phosphate and Adenosine-5'-Triphosphate Uptake by Cyanobacteria and Heterotrophic Bacteria in the Sargasso Sea. *Limnol. Oceanogr.* 56, 323–332. doi: 10.4319/lo.2011.56.1.0323

Mills, M. M., Ridame, C., Davey, M., La Roche, J. and Geider, R. J. (2004). Iron and Phosphorus Co-Limit Nitrogen Fixation in the Eastern Tropical North Atlantic. *Nature* 429, 292–294. doi: 10.1038/nature02550

Moisander, P. H., Beinart, R. A., Voss, M. and Zehr, J. P. (2008). Diversity and Abundance of Diazotrophic Microorganisms in the South China Sea During Intermonsoon. *ISME. J.* 2, 954–967. doi: 10.1038/ismej.2008.51

Moisander, P. H., Zhang, R., Boyle, E. A., Hewson, I., Montoya, J. P. and Zehr, J. P. (2012). Analogous Nutrient Limitations in Unicellular Diazotrophs and Prochlorococcus in the South Pacific Ocean. *ISME. J.* 6, 733–744. doi: 10.1038/ismej.2011.152

Moore, L. R., Ostrowski, M., Scanlan, D. J., Feren, K. and Sweetsir, T. (2005). Ecotypic Variation in Phosphorus-Acquisition Mechanisms Within Marine Picocyanobacteria. *Aquat. Microb. Ecol.* 39, 257–269. doi: 10.3354/ame039257

Müller, W. E. G., Schröder, H. C. and Wang, X. (2019). Inorganic Polyphosphates As Storage for and Generator of Metabolic Energy in the Extracellular Matrix. *Chem. Rev.* 119, 12337–12374. doi: 10.1021/acs.chemrev.9b00460

Orchard, E. D., Ammerman, J. W., Lomas, M. W. and Dyhrman, S. T. (2010a). Dissolved Inorganic and Organic Phosphorus Uptake in Trichodesmium and the Microbial Community: The Importance of Phosphorus Ester in the Sargasso Sea. *Limnol. Oceanogr.* 55, 1390–1399. doi: 10.4319/lo.2010.55.3.1390

Orchard, E. D., Benitez-Nelson, C. R., Pellechia, P. J., Lomas, M. W. and Dyhrman, S. T. (2010b). Polyphosphate in Trichodesmium From the Low-Phosphorus Sargasso Sea. *Limnol. Oceanogr.* 55, 2161–2169. doi: 10.4319/lo.2010.55.5.2161

Orchard, E., Webb, E., and Dyhrman, S. (2003). Characterization of Phosphorus-Regulated Genes in Trichodesmium spp. *The Biological Bulletin*, 205 (2), 230–231. doi: 10.2307/1543268

Palter, J. B., Lozier, M. S., Sarmiento, J. L. and Williams, R. G. (2011). The Supply of Excess Phosphate Across the Gulf Stream and the Maintenance of Subtropical Nitrogen Fixation. *Global Biogeochem. Cycles* 25, 1–14. doi: 10.1029/2010GB003955

Polerecky, L., Adam, B., Milucka, J., Musat, N., Vagner, T. and Kuypers, M. M. M. (2012). Look@ NanoSIMS–a Tool for the Analysis of nanoSIMS Data in Environmental Microbiology. *Environ. Microbiol.* 14, 1009–1023. doi: 10.1111/j.1462-2920.2011.02681.x

Pujo-Pay, M. and Raimbault, P. (1994). Improvement of the Wet-Oxidation Procedure for Simultaneous Determination of Particulate Organic Nitrogen and Phosphorus Collected on Filters. *Mar. Ecol. Ser.* 105, 203. doi: 10.3354/meps105203

Rousselet, L., de Verneil, A., Doglioli, A. M., Petrenko, A. A., Duhamel, S., Maes, C., et al. (2018). Large-To Submesoscale Surface Circulation and its Implications on Biogeochemical/Biological Horizontal Distributions During the OUTPACE Cruise (Southwest Pacific). *Biogeosciences* 15, 2411–2431. doi: 10.5194/bg-15-2411-2018

Saito, M. A., Bertrand, E. M., Dutkiewicz, S., Bulygin, V. V., Moran, D. M., Monteiro, F. M., et al. (2011). Iron Conservation by Reduction of Metalloenzyme Inventories in the Marine Diazotroph Crocosphaera Watsonii. *Proc. Natl. Acad. Sci.* 108, 2184–2189. doi: 10.1073/pnas.1006943108

Sañudo-Wilhelmy, S. A., Kustka, A. B., Gobler, C. J., Hutchins, D. A., Yang, M., Lwiza, K., et al. (2001). Phosphorus Limitation of Nitrogen Fixation by Trichodesmium in the Central Atlantic Ocean. *Nature* 411, 66–69. doi: 10.1038/35075041

Sanz-Luque, E., Bhaya, D. and Grossman, A. R. (2020). Polyphosphate: A Multifunctional Metabolite in Cyanobacteria and Algae. *Front. Plant Sci.* 11. doi: 10.3389/fpls.2020.00938

Smith, D. C. and Azam, F. (1992). A Simple, Economical Method for Measuring Bacterial Protein Synthesis Rates in Seawater Using 3H-Leucine. *Mar. Microb. Food webs* 6, 107–114.

Stenegren, M., Caputo, A., Berg, C., Bonnet, S. and Foster, R. A. (2018). Distribution and Drivers of Symbiotic and Free-Living Diazotrophic Cyanobacteria in the Western Tropical South Pacific. *Biogeosciences* 15, 1559–1578. doi: 10.5194/bg-15-1559-2018

Tilliette, C., Taillandier, V., Bouruet-Aubertot, P., Grima, N., Maes, C., Montanes, M., et al (2022). DFe Patterns Impacted by Shallow Hydrothermal Sources Along a Transect Through the Tonga-Kermadec Arc. Under Consid. *Glob. Biogeochem. Cycles.* doi: 10.1002/essoar.10510604.1

Van Wambeke, F., Bonnet, S., Moutin, T., Raimbault, P., Alarcón, G. and Guieu, C. (2008). Factors Limiting Heterotrophic Bacterial Production in the Southern Pacific Ocean. *Biogeosciences* 5, 833–845. doi: 10.5194/bg-5-833-2008

Van Wambeke, F., Gimenez, A., Duhamel, S., Dupouy, C., Lefevre, D., Pujo-Pay, M., et al. (2018). Dynamics and Controls of Heterotrophic Prokaryotic Production in the Western Tropical South Pacific Ocean: Links With Diazotrophic and Photosynthetic Activity. *Biogeosciences* 15, 2669–2689. doi: 10.5194/bg-15-2669-2018

Wanner, B. L. and McSharry, R. (1982). Phosphate-Controlled Gene Expression in Escherichia Coli K12 Using Mudl-Directed lacZ Fusions. *J. Mol. Biol.* 158, 347–363. doi: 10.1016/0022-2836(82)90202-9

Webb, E. A., Jakuba, R. W., Moffett, J. W. and Dyhrman, S. T. (2007). Molecular Assessment of Phosphorus and Iron Physiology in Trichodesmium Populations From the Western Central and Western South Atlantic. *Limnol. Oceanogr.* 52, 2221–2232. doi: 10.4319/lo.2007.52.5.2221

Wilkins, A. S. (1972). Physiological Factors in the Regulation of Alkaline Phosphatase Synthesis in Escherichia Coli. *J. Bacteriol.* 110, 616–623. doi: 10.1128/jb.110.2.616-623.1972

Wu, J., Sunda, W., Boyle, E. A. and Karl, D. M. (2000). Phosphate Depletion in the Western North Atlantic Ocean. *Sci. (80-. ).* 289, 759–762. doi: 10.1126/science.289.5480.759

Young, C. L. and Ingall, E. D. (2010). Marine Dissolved Organic Phosphorus Composition: Insights From Samples Recovered Using Combined Electrodialysis/Reverse Osmosis. *Aquat. Geochemistry.* 16, 563–574. doi: 10.1007/s10498-009-9087-y

**Conflict of Interest:** The authors declare that the research was conducted in the absence of any commercial or financial relationships that could be construed as a potential conflict of interest.

**Publisher's Note:** All claims expressed in this article are solely those of the authors and do not necessarily represent those of their affiliated organizations, or those of the publisher, the editors and the reviewers. Any product that may be evaluated in this article, or claim that may be made by its manufacturer, is not guaranteed or endorsed by the publisher.

*Copyright © 2022 Filella, Riemann, Van Wambeke, Pulido-Villena, Vogts, Bonnet, Grosso, Diaz, Duhamel and Benavides. This is an open-access article distributed under the terms of the Creative Commons Attribution License (CC BY). The use, distribution or reproduction in other forums is permitted, provided the original author(s) and the copyright owner(s) are credited and that the original publication in this journal is cited, in accordance with accepted academic practice. No use, distribution or reproduction is permitted which does not comply with these terms.*